J Appl Phycol (2009) 21:529–541
DOI 10.1007/s10811-009-9403-3

SunCHem: an integrated process for the hydrothermal production of methane from microalgae and CO_2 mitigation

Anca G. Haiduc · Martin Brandenberger · Sébastien Suquet · Frédéric Vogel · Rizlan Bernier-Latmani · Christian Ludwig

Received: 31 July 2008 / Revised and accepted: 8 January 2009 / Published online: 12 February 2009

Abstract We describe a potential novel process (SunCHem) for the production of bio-methane via hydrothermal gasification of microalgae, envisioned as a closed-loop system, where the nutrients, water, and CO_2 produced are recycled. The influence on the growth of microalgae of nickel, a trace contaminant that might accumulate upon effluent recycling, was investigated. For all microalgae tested, the growth was adversely affected by the nickel present (1, 5, and 10 ppm). At 25 ppm Ni, complete inhibition of cell division occurred. Successful hydrothermal gasification of the microalgae *Phaeodactylum tricornutum* to a methane-rich gas with high carbon gasification efficiency (68–74%) and C1–C3 hydrocarbon yields of 0.2 $g_{C1–C3}/g_{DM}$ (DM, dry matter) was demonstrated. The biomass-released sulfur was shown to adversely affect Ru/C catalyst performance. Liquefaction of *P. tricornutum* at short residence times around 360°C was possible without coke formation.

Keywords Biofuel · Hydrothermal gasification · CO_2 mitigation · Nutrient recycling · Bio-SNG

Paper presented at the 3rd Congress of the International Society for Applied Phycology, Galway.

A. G. Haiduc (✉) · S. Suquet · R. Bernier-Latmani · C. Ludwig
Ecole Polytechnique Fédérale de Lausanne (EPFL) ENAC-ISTE,
1015 Lausanne, Switzerland
e-mail: anca.haiduc@epfl.ch

M. Brandenberger · F. Vogel · C. Ludwig
General Energy Research Department,
Laboratory for Energy and Materials Cycles,
Paul Scherrer Institut (PSI),
5232 Villigen PSI, Switzerland

Introduction

The world's energy needs are presently covered mainly by fossil fuels. The numerous problems related to their exploitation (air pollution, greenhouse gas emissions, and related climate change) and their depleting supply, make the finding of alternatives to their use a very pressing issue. Bioenergy derived from biomass could offer a cost-effective alternative to the use of fossil fuels and might lead to reduced net CO_2 emissions (Hall et al. 1991). However, the use of bioenergy requires large areas of land to intercept incoming solar radiation, and the total amount of energy that can be obtained from these sources is limited. The use of biomass for biofuels production has recently been the subject of much debate especially in relation to fuel–food competition and the associated increases in food prices.

In recent years, a great deal of research has been carried out on various concepts proposing the use of microalgae for energy and biofuel (mainly biodiesel) production coupled to CO_2 fixation as a greenhouse gas mitigation strategy (Hase et al. 2000; Nagase et al. 2001; Nakajima et al. 2001; Wang 2008). Compared to other types of biomass, e.g., corn or soybeans that need fertile land to grow, microalgae are attractive as they can be grown in photobioreactors (open or closed) on marginal land, thus offering the opportunity to utilize land resources that are unsuited for other uses. Land use needs for microalgae complement rather than compete with other biomass-based fuel technologies. Microalgae are amongst the most photosynthetically efficient organisms and many are more productive than land plants and macroalgae (Benemann et al. 1980; Aaronson and Dubinsky 1982). The maximum theoretical photosynthetic efficiency, defined as the fraction of light energy fixed as chemical energy during autotrophic growth, has been estimated to be 9% for microalgae (Wijffels 2008), in

contrast to only 6% for higher plants (Pirt 1980; Bassham 1977), though in practice the values are significantly lower (Richmond 2004). Yields obtained in open ponds have been comparable to those obtained in conventional tropical agriculture (25–30 t ha^{-1} $year^{-1}$), while in closed photobioreactors much higher productivities have been reported (50–150 t ha^{-1} $year^{-1}$), although in general these were relatively small-scale experiments of short duration (Carlsson et al. 2007).

One of the key technical and economical challenges that needs to be overcome before the large-scale introduction of microalgae technology for biofuel production and greenhouse gas mitigation is the efficient conversion of algae biomass to biofuels. This paper describes our current work directed towards eventual demonstration of the technical and economical feasibility of an innovative process ("SunCHem") for sustainable production of bio-fuels (methane and optionally hydrogen) via hydrothermal (HT) processing of microalgal biomass and capture and recycling of CO_2.

We have previously demonstrated the feasibility of hydrothermal gasification of swine manure and woody biomass to produce synthetic natural gas (SNG; Waldner and Vogel 2005; Vogel and Hildebrand 2002). The wood was completely gasified in a batch reactor without forming tars or coke. Methane yields obtained at 400°C and 30 MPa with a Raney Ni catalyst corresponded to the thermodynamic equilibrium (49% vol. methane). A new continuous test rig has been set up at the Paul Scherrer Institut (PSI) that allows the demonstration of the whole biomass-to-SNG process chain at a throughput of 1 kg/h (Fig. 1).

While the two main parts of the process, i.e., growing of microalgae and hydrothermal processing of biomass have been previously studied independently, coupling of these two parts into a sustainable process is a novel concept. As such, the linking of these subsystems into one continuous process will present several challenges. The major difficulties in the SunCHem process are expected to stem from its closed-loop nature, especially in relation to water and nutrient recycling. Upon continuous operation, the recycled water from the process becomes progressively enriched with a variety of trace contaminants which could affect the overall process. Therefore, the aim of our experimental work was: (1) to investigate the influence of nickel, a trace contaminant that may be present in the effluent recycled from the HT process as a result of reactor wall corrosion, on the growth of algae, and (2) to study the efficiency of HT catalytic gasification of the diatom *Phaeodactylum tricornutum*, a microalgae of potential interest for our process.

This paper is organized in two parts. The first part provides a description of the envisaged SunCHem process and outlines its potential advantages compared to conventional processes for biomass conversion to methane. The second part describes our experimental work on assessing the feasibility of effluent recycling on the microalgae biomass growth, and on the HT gasification of microalgae biomass (see above).

The SunCHem process

SunCHem is a process for the production of biofuels (methane, and optionally hydrogen) via hydrothermal processing of microalgae. The energy stored in methane comes from sunlight, through the efficient photosynthetic production of algal biomass. The primary carbon source for microalgae is CO_2 from atmospheric as well as anthropogenic sources, e.g., CO_2 from exhaust gases of fossil power plants. Using CO_2 from stack gases to produce biofuels (e.g., methane) serves the additional purpose of preventing the

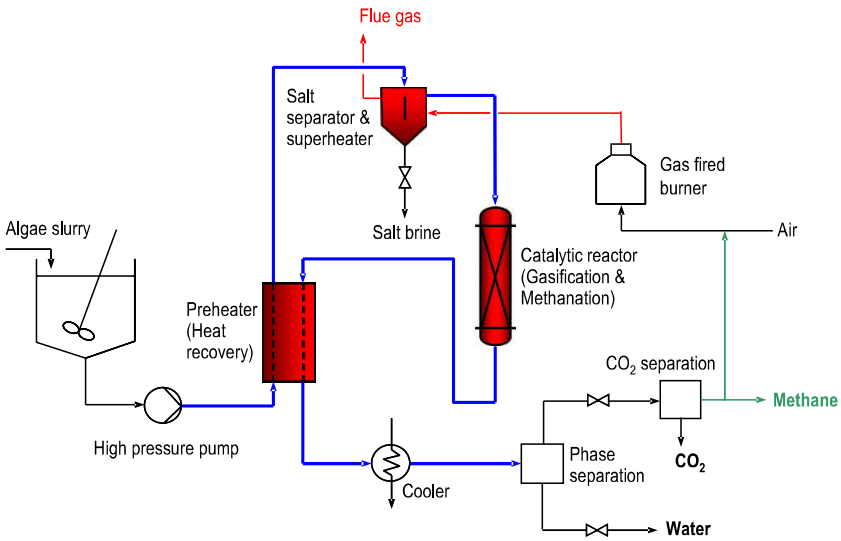

Fig. 1 Sketch of the catalytic hydrothermal gasification process developed at PSI

release of part of the CO_2 generated otherwise by fossil fuel combustion. The SunCHem process might offer a valuable CO_2 mitigation strategy that could bring additional economical and environmental benefits. For further improvement of the overall economics of the process, the coupled synthesis of high-value chemical(s) by the microalgae is an integral part of our process.

A simplified scheme of the envisaged process is presented in Fig. 2. The process consists of five steps. The first step is concerned with the production of biomass in photobioreactors (PBR) or open ponds. The photosynthetic microalgae fix CO_2 and transform it into biomass and O_2 by photosynthesis. In the second step, excess water is removed mechanically from the biomass to approx. 15–20% wt. dry mass. The separated water containing a part of the nutrients is recycled to the algae growth system. The biomass slurry is then liquefied hydrothermally by heating it up to a temperature of 400–450°C under a pressure of 30 MPa, and the remaining nutrients are separated from the liquefied slurry for reuse as nutrients. In the fourth step, the stream containing the organic fraction and the water is catalytically gasified under hydrothermal conditions to methane (Bio-SNG) as the major product. In a last step, the concentrated CO_2 is separated from the product gas and recycled to the photobioreactor. Part of the methane is used to cover the heating needs of the process. This process is proposed to be a closed-loop system with respect to water and nutrients, including nitrogen and phosphorus.

Biofuel products

A variety of biofuels (e.g., methane, biodiesel, bioethanol) can potentially be produced from microalgae biomass. Recently, a great deal of research has been dedicated to the production of biodiesel from microalgae as described in Chisti (2007). Fatty acids (FA) are extracted from strains with high FA content (20–50%) and converted to biodiesel via chemical transesterification reactions. At the present stage, biodiesel production from microalgae is faced with numerous problems, especially related to the overall lipid and algal productivities, the difficulties in the extraction process, and the high energy use (Hu et al. 2008; Wijffels 2008).

Methane, a versatile energy carrier, is an attractive conversion product of microalgae biomass obtained either through anaerobic digestion (Golueke and Oswald 1963) with 25–35% thermal efficiency (Yoshida et al. 2003) or via other pathways with high efficiency (>70% thermal efficiency, expressed as the heating value of the net methane produced to the heating value of the biomass in the feed; Zwart and Boerrigter 2005) (Table 1). Upon purification, methane can be distributed via the existing natural gas-specific infrastructure, resulting in significantly reduced handling costs and ensuring widespread acceptance by potential consumers of renewable fuels.

Hydrothermal gasification

Typically, conversion of organic biomass to methane can be achieved via biochemical (enzymatic) or thermochemical processes (Cantrell et al. 2008; Wang 2008). An overview of some typical biochemical and thermochemical processes for the conversion of biomass to SNG is given in Table 1. *Biochemical* conversion through methanogenesis (biogas production) is well suited for wet biomass feeds. Although conventional biogas plants based on anaerobic digestion are simple to operate, they have two major drawbacks: they cannot completely convert the biomass to methane, leaving behind unconverted organic material (thermal efficiency

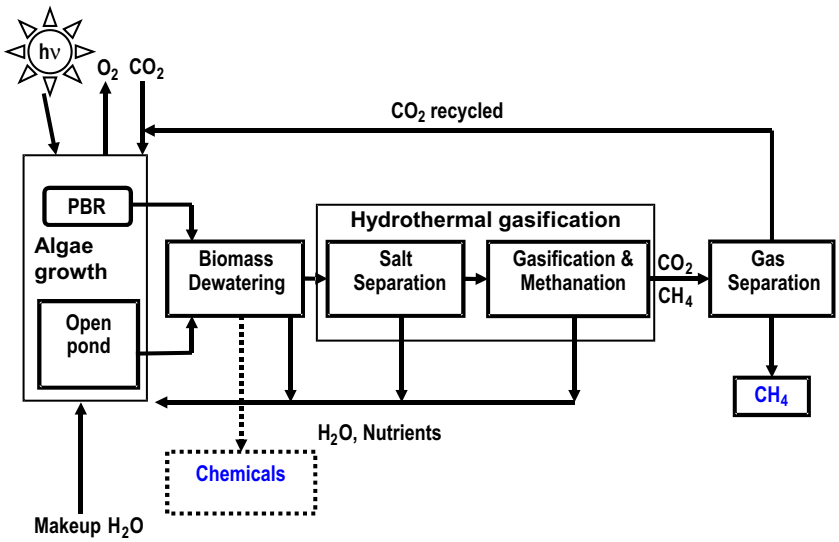

Fig. 2 Simplified scheme of the envisaged SunCHem process for the production of methane (and high-value chemicals) using microalgae. *PBR* Photobioreactor

Table 1 Overview of main characteristics for some typical biochemical and thermochemical processes for biomass conversion to SNG

Characteristic	Conventional gasification & methanation	Anaerobic digestion	Hydrothermal gasification
Feed type	Wood, grass (w_{water} < 15%)	Manure, household residues, sewage sludge, marine algae	Most wet types (w_{water} > 60%)
Thermal efficiency (biomass to SNG)	54–58%[b] (absolutely dry wood)	25–35%[c] (<8 wt % DM manure)	62–71%[d] (manure, wood)
Residence time[a]	<10 min.	20–33 days[c,e]	<30 min.
Technological readiness	Good (PDU 1 MW_{SNG} in Güssing 2008)	Very good (commercially available)	R&D (PDU planned 2010)
Advantages	High efficiency for dry biomass, close to commercialization	Established commercialized, fertilizer by-product	Full conversion, high efficiency, fertilizer by-product
Drawbacks	Low efficiency for wet biomass	Residues, low efficiency, plant size, requirement of co-substrates	Technical barriers to be solved

[a] "Travelling" time through the whole plant
[b] Duret et al. (2005)
[c] Yoshida et al. (2003)
[d] Luterbacher et al. (2009)
[e] Samson and Leduy (1982)

25–35%), and they require long residence times (days, weeks or even months; Yoshida et al. 2003; Samson and Leduy 1982), and hence large reactors for larger scale plants. By contrast, *thermochemical* conversion (TCC) processes are fast, with residence times on the order of minutes or even seconds, thus resulting in reduced footprint requirements (Cantrell et al. 2008). However, *conventional thermal gasification and methanation* requires a dry biomass feed (at least 90% wt. dry mass). As a result, it is unsuitable for wet biomass such as microalgae, because drying the biomass to 90% dry mass is energy intensive and would reduce the overall thermal efficiency to uneconomical levels.

The innovative approach taken in this project is to treat the relatively high water content slurry of algal biomass in an integrated hydrothermal process wherein nutrients are separated and CH_4 is produced. The hydrothermal process has inherent advantages relative to conventional gasification methods. The biomass slurry is gasified under pressure, but at temperatures much lower (ca. 400°C) than typical gasification temperatures (800–900°C). By doing so, there is *no need to dry the biomass* prior to conversion, as gasification in a hydrothermal environment (sub- or supercritical water) is particularly suited for converting *wet biomass* into a fuel gas with a high heating value (Vogel et al. 2007). The process becomes efficient starting at ca. 15% wt. dry mass, in contrast to other TCC technologies. This aspect is of particular interest as microalgae have a high moisture content (0.5–1 g dry-cell L^{-1}, corresponding to 99.95–99.9% water). Performing the gasification above the critical point of water (374°C, 22.1 MPa) will also *prevent tar and char formation* (Modell 1985; Vogel 2009), which is one of the main factors responsible for reducing the efficiency of biomass gasification processes. Avoiding tar and char formation is possible due to the properties of water in the supercritical region that make it a particularly suitable solvent for this process. The dielectric constant, which is a measure of the solvent's polarity, decreases drastically in this region, water behaving consequently like a non-polar solvent. This property might be further exploited for the *separation of nutrient salts* contained in the biomass, which can be recovered as concentrated brine and then further recycled and reused for the growth of algae (Schubert et al. 2008). The possibility to recover the nutrients in the hydrothermal process is very important as the microalgae exhibit high contents of N and P, about 10 and 1%, respectively, on a dry weight basis, several-fold higher than those of higher plants. For the HT process, the presence of salts should also be avoided, as these have been found to deactivate the catalyst and cause corrosion (Waldner et al. 2007). The hydrothermal process uses no organic solvents, the process being basically a *water treatment*. Furthermore, *high thermal process efficiencies* can be reached as shown in Table 1. The process can be *run fast*, with typical residence times of the order of minutes or even seconds for *complete gasification* of the organic matter, thus requiring reduced reactor volumes. The residual organics content in the effluent is usually very low (reduction of organic carbon > 99%; Peterson et al. 2008; Matsumura et al. 2005).

Theoretical and experimental evidence (Kruse 2008; Matsumura et al. 2005; Vogel 2009) indicates that the use of relatively low temperatures (350–500°C) for the hydrothermal gasification of biomass favors methane over

hydrogen formation. A catalyst is required at these lower temperatures for enhancing the reaction kinetics and achieving high levels of carbon conversion to methane gas. Metal-based heterogeneous catalysts were shown to significantly improve gasification efficiency under these conditions (Peterson et al. 2008). The range of suitable metals that can be used is limited, as most metals will undergo oxidation and/or dissolution in the hot-water environment. Typical catalyst supports, e.g., silica and γ-alumina, cannot be used, as they will be severely degraded under the harsh conditions of the supercritical water. During the last 15 years, new catalyst formulations have been developed that use combinations of stable metals such as ruthenium (Ru), or nickel (Ni) bimetallics, and stable supports such as titania, zirconia, or carbon (Elliott et al. 2006; Antal et al. 2000; Waldner et al. 2007; Peterson et al. 2008; Vogel 2009).

Nickel effects on algae

It has been previously reported that at micromolar levels nickel is toxic to a variety of algae, invertebrates, and fish (Mandal et al. 2002; Nriagu 1980; Bielmyer et al. 2006). Several studies exist on the toxicity of nickel to algae and on the bioconcentration of nickel by brown algae and by cyanobacteria and green algae (Wang and Wood 1984; Bordons and Jafre 1987; Wong et al. 2000). Exposure of various species of microalgae to nickel was shown to negatively affect cell division resulting in reduced growth rates (Nriagu 1980). A review of the literature showed that nickel toxicity seems to be related to its concentration, speciation, presence of competing ions, but also on the type and physiological characteristics of microalgae (Fezy et al. 1979; Spencer and Greene 1981; Lustigman et al. 1995; Mandal et al. 2002). However, the results reported in the literature on nickel toxicity are inconsistent due to variability in culture conditions. The reported minimum lethal doses for nickel poisoning, even within individual species, often vary by an order of magnitude (Wang and Wood 1984).

The experimental work was focused on investigating: (1) the growth of algae in the presence of nickel, a trace contaminant likely to be present in the HT effluent recycled to the PBR, and (2) the catalytic hydrothermal gasification of the microalga *Phaeodactylum tricornutum*.

Materials and methods

Influence of nickel on microalgae growth

One important question that needed to be addressed was how the trace contaminants contained in the recycled effluent would affect algae growth. Due to the harsh conditions used during the hydrothermal treatment (400°C, 30 MPa), metals may be slowly released due to catalyst leaching and reactor wall corrosion. As the effluent solution from this process is recycled back into the PBR, the potential accumulation of these metals during the continuous operation of the system could negatively affect the growth of microalgae. Nickel was a trace contaminant identified in the HT effluent, most probably arising from wall corrosion of the batch steel reactor used during the HT gasification experiments (for details on the characteristics of the steel reactor, see below).

Test organisms and culture conditions

All microalgae strains were obtained from the Culture Collection of Algae at Göttingen University (SAG). Both green algae (eukaryotes) and cyanobacteria (prokaryotes) were used in this study. The eukaryotic strains were *Chlorella sorokiniana* (SAG 211–8k), *Chlorella vulgaris* (SAG 211–11b) *Scenedesmus vacuolatus* (SAG 211–8b), and *Dunaliella bioculata* (SAG 19–4), whereas the prokaryotic strain was *Synechococcus leopoliensis* (SAG 1402–1). The eukaryotes were grown in proteose peptone (PP), the prokaryotes in BG11 media prepared by dilution of the concentrated powder supplied by Sigma-Aldrich and *D. bioculata* in a growth medium described by Grobbelaar (2004) containing KNO_3 (0.505 g L^{-1}), $K_2HPO_4 \cdot 3\ H_2O$ (0.014 g L^{-1}), $MgSO_4 \cdot 7\ H_2O$ (1.2 g L^{-1}), $MgCl_2 \cdot 4\ H_2O$ (0.1 g L^{-1}), $CaCl_2 \cdot 2\ H_2O$ (0.033 g L^{-1}), $NaHCO_3$ (1.7 g L^{-1}), NaCl (117.0 g L^{-1}), Tris-HCl (6 g L^{-1}), H_3BO_4 (6 μg L^{-1}), $ZnCl_2$ (14 μg L^{-1}), $CoCl_2 \cdot 6\ H_2O$ (4.8 μg L^{-1}), with final pH adjusted to 7.5. The microalgae were grown in an incubator (Gallenkamp) under controlled and constant temperature (optimum temperature as recommended by supplier, variable for each strain) and a light intensity of 44 Wm^{-2} with a light/dark cycle of 16/8 h. The growth curve for each species was followed to identify the lag, exponential, stationary, and decline phases. Although all the manipulations were carried out under sterile conditions, it is notoriously difficult to obtain and maintain axenic cultures of microalgae. Ultrapure (MiliQ) water was used throughout the work.

Analytical methods

The growth of the microalgae was followed by direct microscope counting of cell numbers from each solution using a counting chamber (Improved Neubauer Bright) and a Zeiss AXiolab light microscope. Cell counting was done at 24-h intervals with the first count at 48 h for a total experimental time of 140 h. To obtain representative samples, the algal suspensions were homogenized before sampling by vigorous swirling on a vortexer. Total organic carbon was determined using a Shimadzu TOC 5000

instrument. The pH value of the cultures was measured at the beginning and at the end of each experiment (Thermo Orion 3-Star). Stock solutions containing nickel were prepared by dissolving the required amount of $NiSO_4 \cdot 6\ H_2O$ in water. Nickel concentrations in solution were measured at the beginning and at the end of experiments using ICP-OES (Perkin-Elmer Plasma 2000 Optima3300 DV).

Experimental procedure

Batch-grown cells were harvested in the exponential phase (3 days) and inoculated in 250-mL Erlenmeyer flasks containing 100 mL nutrient medium to reach a final concentration of 10^5 cells mL^{-1}. Aliquots from the heat-sterilized nickel stock solution were added to the flasks and diluted to achieve final concentrations of 1, 5, 10, and 25 ppm. The concentrations of the metal solutions were chosen to bracket the values expected as a result of recirculation of the nutrient medium from the hydrothermal gasification process, as suggested by our preliminary work. Each experiment was performed in duplicate, and positive and negative controls were used. For the positive control, the microalgae were grown in nutrient medium without addition of the metal solution. The negative control consisted of the nutrient medium and the metal solution without microalgae cells and was used to check for possible medium contamination. Duplicate 1-mL aliquots were taken from each flask and cells were counted. The mean value for these two readings was reported.

Catalytic HT gasification experiments of the microalgae *Phaeodactylum tricornutum*

Screening experiments were conducted to test the gasification of the microalga *P. tricornutum* under supercritical water conditions (~400°C, 30 MPa) in a stainless steel batch reactor. This particular set of conditions (i.e., 400°C, 30 MPa, and 60 min for the full gasification experiments) was known from prior experiments with other biomass to yield full conversion of the organic fraction to a methane-rich gas. The goal of our study was to assess the performance of a carbon-supported ruthenium catalyst (2% wt. Ru on activated carbon from Engelhard) that we have used successfully in the earlier studies (Waldner et al. 2007; Vogel et al. 2007). Some runs were performed in the absence of the catalyst to check for coke formation and to obtain a baseline conversion.

High pressure batch reactor system and gas analysis

The catalytic hydrothermal gasification of *P. tricornutum* was conducted in a small batch reactor system developed at PSI with a total internal volume of approximately 30 mL. The high-pressure sections of the reactors were constructed with standard parts from HiP (High Pressure Equipment, USA). The reactor consisted of a high-pressure 316 stainless steel tube (25.4 mm o.d. × 14.3 mm i.d., length 152.4 mm). A sheathed 1.6-mm K-type thermocouple was fitted to the bottom, in contact with the fluid inside the reactor. Additionally, a second K-type thermocouple measured the outside reactor wall temperature at the top of the reactor to detect temperature gradients in the reactor. A 316 stainless steel capillary tube (3.2 mm o.d. × 1.6 mm i.d., length 223 mm) was connected to the reactor tube by a high-pressure union, thus linking the hot part of the reactor with the cold upper part and the gas sampling system. The gas sampling system consisted of two high pressure valves in a sequence. Gas samples could be taken with a gas sampling bag (volume 1 L, SKC). The gas samples were analyzed off-line with a gas chromatograph (Agilent 6890).

Catalyst characterization

A commercial 2% wt. ruthenium on granular coconut carbon catalyst (Sample Code: 44915, Lot: 11829) was obtained from Engelhard-BASF (Italy). Characterization of the fresh 2% Ru/C catalyst has been described in detail by Waldner (2007).

Biomass source & characterization

Phaeodactylum tricornutum was obtained as 13% wt. DM (dry matter) concentrated microalgae suspension from a commercial microalgae producer (Subitec, Germany). The elemental composition of *P. tricornutum* was determined at ETH Zurich (Laboratory for Organic Chemistry). The ash content was determined in duplicate at 550°C for 1 h in a furnace (Nabertherm C6D), cooled down in a desiccator, weighed and again treated at 550°C for 30 min until the change in weight was less than 4% or 50 mg, according to method 2540 G (Eaton et al. 2005). Elemental composition and ash content are summarized in Table 2.

Experimental procedure

Water and biomass were mixed to yield the desired feed concentration (2.5, 5, 10, and 13% wt., respectively). The amount of catalyst corresponding to the desired ratio of catalyst to biomass was then added, and the mixture was transferred into the reactor. The reactor tube was closed

Table 2 Elemental composition and ash content of *P. tricornutum* in % wt. on a dry basis

C	H	O	N	S	Ash
57.03	7.46	24.97	8.00	1.28	12.45

tightly with the help of a torque wrench and connected to the capillary tube. Air was removed by evacuating the apparatus with a vacuum pump and the reactor was flushed twice with argon before each experiment. Before starting the gasification experiments, the reactor was pressurized with 2.0–4.2 MPa of argon to avoid water evaporation and drying out of the biomass slurry during heat-up. Argon also served as a leak test (see argon mass balance closure in Table 3).

The reaction was initiated by the immersion of the reactor assembly into a preheated fluidized sand bath (Techne SBL-2D). The desired reaction temperature T_{end} was reached in less than 10 min after immersion. To stop the reaction after a predetermined time, the reactor was lifted out of the fluidized sand bath and quenched in a cold water bath. The pressure inside the reactor and the temperatures were measured and recorded at intervals of 1 s using a LabView™-based data acquisition system.

Liquid sample analysis

Liquid samples were obtained through filtration of the batch reactor content over a membrane filter (regenerated cellulose, pore size 0.45 μm, diam. 47 mm, Schleicher & Schuell Microscience, Germany) with a Sartorius vacuum filtration apparatus (Goettingen, Germany). The TOC (total organic carbon) content of the liquid sample was measured with an IL550 TOC-TN from Hach Lange by the differential method. The pH value of the aqueous samples was measured with color-fixed pH indicator sticks (pH 7–14, Fisherbrand, EU Code: FB33015).

Calculation of the amount of gasified feed carbon and the C1–C3 yield

The yield of methane, ethane, and propane (Y_{C1-C3}) was calculated based on the results of the gas analysis:

$$Y_{C1-C3} = m_{C1-C3}/m_{DM} = f(V,p,X)$$
$$m_{C1-C3} = m(CH_4) + m(C_2H_6) + m(C_3H_8)$$

V stands for the volume of the gas sampling bag and reactor in m^3. Amount of dry biomass is given as m_{DM} (g), whereas the amount of methane, ethane and propane is indicated by m_{C1-C3} (g). p is the ambient atmospheric pressure (MPa) and X designates the percentage of CH_4 + C_2H_6 + C_3H_8 in the product gas (vol %) obtained from GC measurements.

The amount of gasified feed carbon was calculated by the following formula and given as a percentage (%):

$$C_{gas}/C_{feed} = m(C_{gas})/m(C_{feed}) \times 100$$

with $m(C_{gas})$ representing the carbon content of the product gas in grams. The value of $m(C_{gas})$ is calculated based on the amount of moles in the gas phase (mol_{CO2gas}, mol_{COgas}, mol_{CH4gas}, $mol_{C2H6gas}$, $mol_{C3H8gas}$). The dissolved CO_2 in the liquid fraction is indicated by $mol_{CO2dissolved}$. The parameter $mol_{CO2dissolved}$ was strongly affected by the measured pH in the liquid effluent of the reactor, because the solubility of CO_2 is a strong function of the pH. CO_2 from the gasification remains partially in the liquid phase as inorganic carbon (TIC = total inorganic carbon; Table 3). As our batch reactor is a non-stirred system, a considerable uncertainty about how much of the CO_2 is dissolved in the liquid phase exists. $m(C_{feed})$ is the carbon present in the feed calculated from w_C representing the carbon mass fraction of the feed (carbon fraction from *P. tricornutum*) and m_{DM}.

$$m(C_{gas}) = (mol_{CO_2gas} + mol_{CO_2dissolved} + mol_{CH_4gas} + mol_{COgas} + 2 * mol_{C_2H_6gas} + 3 * mol_{C_3H_8gas}) * 12.01g/mol_{Carbon}$$

$$m(C_{feed}) = m_{DM} * w_C$$

Argon mass balance

The ratio Ar_{gas}/Ar_{feed} is the amount of argon recovered after the experiment to the amount of argon added for pressurizing the reactor. Significant deviations from 100% indicate a leakage, losses during gas sampling, or errors in the gas analysis.

An overview of the experimental conditions (catalyst, feed concentration, residence time) used in each run (T1–T6) is given in Table 3.

Results

Influence of nickel on microalgae growth

Comparison of growth curves in the absence vs. presence of nickel (at 10 ppm)

The first result of cell counting is reported at 48 h. The values from cell counting were used to calculate the algae concentrations. Due to the small size of the cyanobacteria (*S. leopoliensis* 0.8–1.5 μm, *Chlorella* sp. 2–10 μm), some difficulties were encountered while counting the cell numbers of *S. leopoliensis*, thus probably resulting in greater counting errors than for the eukaryotes.

Figure 3 shows the growth curves for all algae strains (a) without nickel present versus (b) in the presence of 10 ppm nickel in the nutrient medium. The presence of nickel in the nutrient medium was associated with a decrease in microalgae cell density. The deleterious effect of nickel on algae growth was observed for all strains considered. In the

Table 3 Summary of gasification experiments with *P. tricornutum*

Run	Catalyst	Feed conc. %wt.	$n_S/n_{Ru,sfc}$ mol/mol	RT min.	C_{gas}/C_{feed} % (mol/mol)	CH_4 %vol.	C_2H_6 %vol.	C_3H_8 %vol.	CO_2 %vol.	CO %vol.	H_2 %vol.	$Y_{C1–C3}$ $g_{C1–C3}/g_{DM}$	Ar_{gas}/Ar_{feed} % (mol/mol)	TOC mg/L	TIC mg/L
T1	Ru/C	5.1	0.3	67	74	34.4	2.0	0.7	56.7	0.6	5.5	0.204	99	217	2,631
T2	–	13.0	–	13	4	n.d.	n.d.	n.d.	100.0	n.d.	n.d.	0.000	98	n.a.	n.a.
T3	Ru/C	13.0	0.8	64	34	46.4	4.2	0.9	40.6	3.3	4.7	0.133	107	n.a.	n.a.
T4	–	10.0	–	12	4	n.d.	n.d.	n.d.	100.0	n.d.	n.d.	0.000	106	18,063	2,044
T5	–	13.0	–	16	8	4.8	2.9	2.9	84.8	4.7	n.d.	0.009	n.a.	20,089	3,020
T6	Ru/C	2.5	0.3	60	68	41.5	n.d.	n.d.	50.5	n.d.	8.0	0.206	97	606	1,392

TOC Total organic carbon, *TIC* total inorganic carbon, *RT* reaction time
n.a. not available, n.d. not detected, (–) does not apply here

absence of nickel (Fig. 3a), the fastest growing alga was *C. sorokiniana*, which achieved cell concentrations one order of magnitude higher than the second fastest strain, *S. leopoliensis*. Lower cell concentrations, by one more order of magnitude, were seen for *D. bioculata*, *C. vulgaris*, and *S. vacuolatus*. After this time, all algae strains showed a leveling off of the growth curve most likely due to depletion of the available nutrients. Although after 140 h the highest cell count was recorded for *S. leopoliensis*, results of TOC (not presented here) showed that its TOC content was in fact much lower than for the other algae, most probably due to its smaller cell size and therefore later onset of nutrient limitation. In the presence of 10 ppm nickel (Fig. 3b), the highest cell count was still recorded for *C. sorokiniana*, nevertheless the concentrations achieved were more than one order of magnitude lower than those recorded in the absence of nickel. The same trend was observed for *D. bioculata* and *S. vacuolatus* whose growth was also depressed by about an order of magnitude in the presence of nickel. The most sensitive strain in our study appeared to be *S. leopoliensis* for which no growth was observed in the presence of nickel in solution for the entire duration of the experiment.

Comparison of growth curves at different nickel concentrations

A comparison of the algal growth curves in the presence of nickel at 1, 5, 10, and 25 ppm showed that the higher the nickel concentration in the nutrient medium, the lower the algal cell densities recorded. Figure 4 shows a comparison of the growth curves of *S. vacuolatus* at various nickel concentrations. The observed trend was typical for all microalgae studied, namely the higher the nickel concentration used, the more pronounced was its inhibitory effect on microalgae growth. At nickel concentrations up to 10 ppm, all microalgae, with the exception of *S. leopoliensis*, continued to grow, albeit at slower rates and resulting in lower total biomass. Furthermore, a nickel concentration of 25 ppm completely inhibited cell division for all microalgae studied and no growth was recorded under these conditions for the entire duration of the experiments.

Catalytic HT gasification experiments of the microalgae *P. tricornutum*

An overview of the experimental results from the catalytic hydrothermal gasification of the microalgae *P. tricornutum* is presented in Table 3 showing the measured gas composition (CH_4, C_2H_6, C_3H_8, CO_2, CO, H_2), the calculated carbon gasification efficiency C_{gas}/C_{feed}, the yield of C1–C3 gases $Y_{C1–C3}$, the mole ratio of sulfur atoms to surface Ru atoms from the catalyst, $n_S/n_{Ru,sfc}$, and the argon mass balance closure Ar_{gas}/Ar_{feed}.

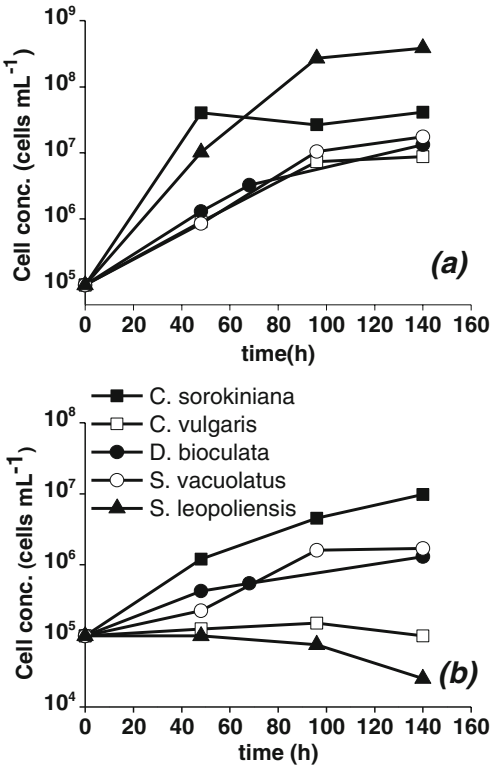

Fig. 3 Comparison of growth curves for the different microalgae strains with **a** no Ni present versus **b** 10 ppm Ni

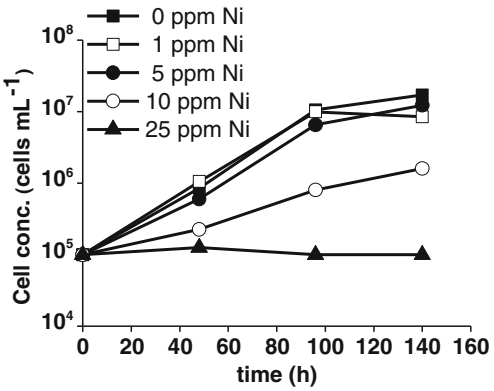

Fig. 4 Comparison of growth curves for *S. vacuolatus* at different Ni concentrations

Carbon gasification efficiency C_{gas}/C_{feed} varied from 4 to 8% in the liquefaction runs (T2, T4, T5), where no catalyst was used, to 34–74% in the runs where the Ru/C catalyst was employed (T1, T3, T6). For runs T2, T4, T5, performed in the absence of the catalyst, the product gas was composed mainly of CO_2. For the other runs where the catalyst was present, the Y_{C1-C3} was lower for run T3 (0.133) compared to runs T1 and T6 which showed similar values (0.204 and 0.206 g_{C1-C3}/g_{DM}).

The gas composition was also different, with a more favorable composition of C1–C3 gases and a lower CO_2 content in run T3 compared to run T1 of 56.7 versus 40.6% vol., respectively. The aqueous phase obtained in both runs T1 and T6 was a clear, transparent liquid. The measured TOC values were 217 ppm and 606 ppm, and the TIC values were 2,631 ppm and 1,392 ppm, for runs T1 and T6, respectively (Table 3).

Runs T4 and T5 were performed in the absence of a catalyst, under two different temperatures and using short residence times, to test the liquefaction and coking of the biomass under these conditions. Run T4, performed at a temperature of 360°C using a residence time of 12 min, yielded a clear yellow liquid, but a few solid particles were still observed after filtration of the reactor content through a cellulose filter. Experiment T5 was performed at a higher temperature, 420°C, and yielded, besides the clear yellow liquid similar to that of run T4, a much larger number of solid particles, some alike and some different in appearance to those obtained in run T4.

Discussion

Influence of nickel on microalgae growth

For all microalgae strains studied, we observed a decrease in the cell densities when nickel was present in the nutrient medium compared to those where nickel was absent. This is in line with the literature reports showing the toxic effects of nickel on microalgae at micromolar levels (Mandal et al. 2002).

In our experiments, we observed that in the presence of nickel at concentrations of up to 10 ppm, microalgae were still viable and cells continued to divide for the entire duration of the experiment (140 h). However, the growth of all strains was reduced in direct correlation with the level of nickel (Figs. 3 and 4). Our findings are in agreement with those of Lee and Lustigman (1996) who showed that nickel concentrations above 10 ppm were deleterious for the growth of the microalgae *Anacystis nidulans*. However, in a previous study, the same group (Lustigman et al. 1995) found that the growth of *Chlorella vulgaris* was slightly stimulated by a nickel concentration of 10 ppm. Similarly, Wong et al. (2000) reported a decrease in the growth rate for two *Chlorella* strains in the presence of up to 40 ppm nickel, which was directly correlated to the concentration of nickel.

At even higher nickel concentrations (i.e., 25 ppm), we observed complete inhibition of cell division for all microalgae strains considered, and a typical curve is shown in Fig. 4 for *S. vacuolatus*. Although in our case the 25 ppm nickel stopped cell division, suspension of the recovered algae cells in fresh sterile medium with no nickel present resulted in new growth, as proved by visual and optical microscopy inspection of the cultures, although no quantitative investigations were undertaken. Likewise, (Wong et al. 2000) reported that the microalgae species tested remained viable after a 24-h exposure to up to 40 mg L^{-1} Ni^{2+}. Moreover, they reported that even after a cyclic exposure to up to 30 ppm nickel (ten 24-h cycles) the microalgae cells remained viable, and started growing when re-suspended in fresh medium (Tam et al. 2001). Lustigman et al. (1995) report a decreased growth for *C. vulgaris* at 25 ppm nickel, while an even higher level of 50 ppm was lethal to the algae, as these subsequently lacked the capacity to recover.

As can be seen in Fig. 3, the strain that was most negatively affected by the presence of nickel in the system was *S. leopoliensis* for which no growth was observed in the presence of 10 ppm nickel in solution for the entire duration of the experiment. The higher sensitivity of *S. leopoliensis*, a cyanobacterium, versus that of the green algae is in accordance with previous literature reports that showed that the prokaryotes (cyanobacteria) were generally more sensitive to nickel toxicity than the eukaryotes (green algae; Wang and Wood 1984). The increased sensitivity of the prokaryote *S. leopoliensis* can be explained by its reduced structural complexity compared to that of the eukaryotes. Another factor that can be partially responsible for this increased sensitivity of the cyanobacteria is the difference in cell size. In our study, *S. leopoliensis*, the algae that had the smallest cell size, was the most

susceptible to the toxic effects of nickel. It is possible that the larger surface area to volume ratios for the smaller sized cells increases the availability of exterior surfaces for Ni^{2+} uptake (Wong et al. 2000).

Nevertheless, no current consensus appears to exist with regard to the differential toxicity of nickel towards green algae versus cyanobacteria. In contrast to our findings, others (Spencer and Greene 1981) reported that cyanobacteria were more tolerant of increased nickel levels than were species of green algae, although the levels investigated were much lower than those in our study (10.2 μmol L^{-1} = 0.6 mg L^{-1}). The apparent greater tolerance to nickel on the part of the cyanobacteria was ascribed to the production of extracellular organic compounds which could detoxify the nickel.

It is generally accepted that, besides its concentration, the speciation of an element is very important in determining its toxicity, bioavailability, bioactivity, transport, distribution, and, thus, its eventual impact in biological systems and the environment. This, in turn, is strongly influenced by the pH. In most aerobic natural waters in the neutral pH range, the free divalent nickel aquo ions i.e. $[Ni(H_2O)_6]^{2+}$ were found to be the dominant species. At the pH and concentrations used in our study (pH 6.5–8.0), nickel exists largely as free ions (Nriagu 1980). This ionic species was reported to have the highest toxicity towards algae (Spencer and Greene 1981).

Although elucidation of the mechanism of nickel toxicity is beyond the scope of this paper, several possibilities are proposed based on the existing literature. The mechanism responsible for the nickel toxicity might be related to surface binding of nickel to functional groups on extracellular muccopolysaccharides (Wang and Wood 1984). This could then act as a selective barrier for other substances, thus impeding nutrient uptake and finally resulting in a reduction of growth (Bordons and Jafre 1987). Similarly to other toxic metals, nickel could also enter cells by ionic or molecular mimicry by employing channels or carriers involved in ionoregulation. In several organisms, nickel has been shown to enter biological cells via the magnesium transporters (Worms and Wilkinson 2007). Moreover, it was suggested that nickel might affect the functioning of polymerases involved in the biosynthesis of DNA, thereby producing abnormal DNA through this mechanism (Cassarett and Doull 1980). For the microalgae *Chlorella*, Rachlin and Grosso (1993) proposed that the toxicity of nickel might be at the level of the plasma membrane, as was the case with cadmium, copper, and cobalt.

Although the factors mentioned above could, at least partially, influence the resistance of various microalgae species to nickel toxic effects, several other factors such as differences in the physiology of microalgae (e.g., lipid content, composition and structure of cell walls) might ultimately affect nickel-uptake and toxicity.

Our investigations showed that for all microalgae the growth was strongly affected by the nickel concentrations. Thus, in our process, it is important to monitor nickel and maintain the concentration at low levels in the effluent that is recirculated to the PBR and used for the algae growth. If the nickel concentration in the effluent approaches 25 ppm, remedial action should be taken through dilution or removal of the metal toxicant (e.g., by ion exchange). Reduction of nickel toxicity through dilution was employed in the work of Tsukahara et al. (2001). In a similar process for low-temperature gasification of microalgae biomass for energy production, they detected high levels of nickel (240 mg L^{-1}) in the effluent solution arising from leaching of the nickel catalyst used. Upon 30-fold dilution, the toxicity of the solution was significantly reduced, so that it could be recycled and reused as the growth medium for the algae after addition of some essential elements.

Catalytic HT gasification experiments of the microalga *P. tricornutum*

Comparison of the different runs performed in the presence of the Ru/C catalyst (T1, T3, and T6) showed that runs T1 and T6 resulted in higher gasification efficiencies (C_{gas}/C_{feed}, mol/mol, expressed in %) than run T3, i.e. 74 and 68% compared to only 34%, respectively. This was most probably due to the higher feed concentration used in run T3 (13% wt.) compared to that used in runs T1 and T6 (5.1% wt. and 2.5% wt. respectively). As a consequence, a higher sulfur-to-catalyst ratio was present in run T3 compared to T1 or T6. Previously, it has been demonstrated that sulfur is also a strong catalyst poison under hydrothermal conditions (Osada et al. 2007; Waldner et al. 2007). Along with other organically-bound heteroatoms, it may be released from the microalgae as a result of the thermal degradation and hydrolysis of the constituent biomolecules. Free heteroatoms have the potential to poison the catalyst if they are not separated from the degraded biomolecules before entering the catalytic reactor (Waldner 2007).

A low catalyst-to-biomass ratio is expected to yield reduced carbon gasification efficiencies because it results in a higher mole ratio of sulfur atoms to surface ruthenium atoms ($n_S/n_{Ru,sfc}$, mol/mol) and thus increased poisoning of the catalyst. In batch experiments, a fraction of the catalyst effectively acts as an adsorbent for sulfur and does not contribute to the catalytic process. Only free surface ruthenium atoms are able to gasify the algal biomass to a gas composed of methane, ethane, propane, hydrogen, carbon monoxide, and carbon dioxide. Accordingly, the higher sulfur-to-catalyst ratio present in run T3 relative to runs T1 and T6 meant that a higher fraction of the Ru/C catalyst was sacrificed by acting as a sulfur adsorbent and not participating in the catalytic reaction. This probably

explains both the reduced carbon gasification efficiency and the lower yield of C1–C3 gases, methane, ethane, and propane ($Y_{C1–C3}$) obtained in run T3 compared to runs T1 or T6 (0.133 vs 0.204 and 0.206 $g_{C1–C3}/g_{DM}$, respectively; Table 3).

Besides gasification efficiency, another parameter of a high practical significance is the yield of C1–C3 gases. Interestingly, although the gasification efficiency and $Y_{C1–C3}$ was lower for run T3, the product gas had a more favorable composition of methane, ethane and propane than T1 or T6 and significantly less CO_2 (40.6 vs 56.7 and 50.5%, respectively). As the catalyst promotes the formation of methane (Vogel et al. 2007) we would expect run T3 to have more carbon dioxide and less C_1–C_3 compounds in the gas phase. However, run T3 has been performed in two steps: in a first step, the algal biomass was liquefied (T2) and, subsequently, it was gasified by adding the catalyst after the liquefaction (T3). During the liquefaction in the absence of a catalyst, the only gaseous product is CO_2. The CO_2 is probably formed from decarboxylation reactions occurring during the heating up of the microalgae–water mixture (Peterson et al. 2008). Removal of the gas phase CO_2 produced during liquefaction (T2) reduces the O/C ratio and increases the H/C ratio of the remaining organic fraction, both favoring the production of methane instead of CO_2, therefore resulting in an increased methane concentration in the gas phase for run T3.

The separate liquefaction (T2) and gasification (T3) should simulate the different stages of our continuous process (Fig. 1), where the biomass is first liquefied before catalytic gasification (Waldner 2007). However, in runs T2 and T3, salts could not be removed between the liquefaction and gasification step, as opposed to the continuous process which uses an integrated salt separator between these steps (Fig. 1).

Runs T1 and T6 show a very similar SNG yield of 0.204 and 0.206 $g_{C1–C3}/g_{DM}$, respectively, for *P. tricornutum*, although the gas composition was different. As the experiments were done in an unstirred batch reactor, a longer residence time would have been probably necessary to reach the complete conversion to methane with the higher feed concentration in run T1. This was furthermore indicated in run T6, where the ethane and propane concentrations were below the detection limit and the concentrations of methane and hydrogen were higher than for run T1.

Runs T1 and T6 yielded a clear, transparent liquid. The total organic content in the aqueous phase was 217 ppm and 607 ppm (Table 3). In comparison, a blank run with only catalyst and water but no biomass present, yielded an NPOC (non-purgeable organic carbon) value of 167 ppm. The total inorganic carbon (TIC) in the liquid effluent increased from 0 ppm before the experiment to 2,631 ppm and 1,392 ppm for T1 and T6, respectively (Table 3). This indicates that most of the algal biomass carbon was either converted to the gas phase or it was present in a dissolved inorganic carbon form in the liquid phase.

Two additional experiments were carried out with *P. tricornutum* in order to assess the liquefaction (T4) and coking (T5) propensity of the algal biomass, without subsequent gasification. Both properties play an important role for the continuous supercritical gasification of algal biomass. Liquefaction is important because it breaks up the cell structure of the algal biomass and releases heteroatoms. It is therefore crucial to completely liquefy the algal biomass so that no unreacted biomass moieties remain. A liquefaction temperature of 360°C was chosen for experiment T4 and the residence time was kept short (12 min including the heating step), thereby simulating typical residence times in continuous plants. (Peterson et al. 2008; Kruse et al. 2005, 2007). After filtration of the reactor content through a cellulose filter, a clear yellow liquid was obtained. Visual inspection of the few particles retained on the filter suggested these to be inorganic aggregates, but this is yet to be confirmed by suitable analytical procedures.

Higher temperatures favor the formation of coke through secondary condensation and polymerization reactions (Peterson et al. 2008). We tested for coke formation at 420°C in experiment T5 as the temperature in the salt separator of our continuous process demonstration unit reaches that value. Filtration of the reactor content yielded a yellow liquid similar to that from experiment T4. However, this time small particles, probably coke, were retained on the filter and a large particle of 2–3 mm remained after thorough washing with methanol. Furthermore, numerous smaller particles, similar to those observed in run T4, were present, although in larger amounts. The presence of C_1–C_3 compounds in the gas phase of run T5 may be due to decarboxylation of acetic acid or decarbonylation of acetaldehyde above the critical point of water (Peterson et al. 2008). By analogy, ethane and propane may have been formed from propionic and butyric acid.

Our experiments showed that the microalgae biomass (*P. tricornutum*) could be successfully gasified in batch experiments to a methane-rich gas. The remaining liquid was clear and transparent with very low organic carbon content (217–607 ppm) and a high gasification efficiency was obtained (68–74% of the feed carbon was recovered in the gas phase). The yield of C_1–C_3 gases was 0.204–0.206 $g_{C1–C3}/g_{DM}$. The adverse effect of sulfur released from the biomass on the Ru/C catalyst's performance was demonstrated. In a continuous process with an efficient inline salt separation (Fig. 1), the catalyst poisoning can be avoided. Liquefaction of *P. tricornutum* at short residence times around 360°C was possible without coke formation; however, at higher temperatures (e.g., 420°C) coke formation may occur.

Although there are still challenges to be tackled before the technical and economical feasibility and net energy production of the SunCHem process is demonstrated, the results obtained in our experiments confirm that SunCHem is a promising process for efficient production of methane through HT catalytic gasification of microalgae biomass. The economics of the process can be improved by coupling it with the extraction of high-value chemicals from microalgae and additionally exploiting its potential CO_2 mitigation capabilities.

Acknowledgments This project is financially supported by VELUX STIFTUNG (project Nr. 405). Technical and analytical support by Jean-David Teuscher, Simona Regenspurg (EPFL), Martin Schubert, Albert Schuler, Johann Regler (PSI) and fruitful discussions with Pilar Junier (EPFL) are greatly acknowledged. The authors are particularly grateful to Samuel Stucki, the initiator of this project, for his continuous support and encouragement.

References

Aaronson S, Dubinsky Z (1982) Mass production of microalgae. Cell Mol Life Sci 38:36–40

Antal MJ, Allen SG, Schulman D, Xu X, Divilio RJ (2000) Biomass gasification in supercritical water. Ind Eng Chem Res 39:4040–4053

Bassham JA (1977) Increasing crop production through more controlled photosynthesis. Science 197:630–638. doi:10.1126/science.197.4304.630

Benemann JR, Koopman BL, Weissman JC, Eisenberg DM, Goebel P (1980) In: Shelef G, Soeder CJ (eds) Algae biomass: production and use. Elsevier, Amsterdam, pp 457–496

Bielmyer GK, Grosell M, Brix KV (2006) Toxicity of silver, zinc, copper, and nickel to the copepod *Acartia tonsa* exposed via a phytoplankton diet. Environ Sci Technol 40(6):2063–2068. doi:10.1021/es051589a

Bordons A, Jafre J (1987) Extracellular adsorption of nickel by a strain of *Pseudomonas sp*. Enzyme Microb Technol 9(12):709–713. doi:10.1016/0141–0229(87)90029–9

Cantrell KB, Ducey T, Ro KS, Hunt PG (2008) Livestock waste to bioenergy generation opportunities. Bioresour Technol 99 (17):7941–7953. doi:10.1016/j.biortech.2008.02.061

Carlsson AS, van Beilen JB, Möller R, Clayton D, Bowles D (eds) (2007) Micro- and macro-algae: utility for industrial applications. Outputs from the EPOBIO project. CPL Press, Newbury, UK, http://www.epobio.net/pdfs/0709AquaticReport.pdf

Cassarett L, Doull J (eds) (1980) Toxicology, 2nd edn. Macmillan, New York

Chisti Y (2007) Biodiesel from microalgae. Biotechnol Adv 25:294–306. doi:10.1016/j.biotechadv.2007.02.001

Duret A, Friedli C, Marechal F (2005) Process design of Synthetic Natural Gas (SNG) production using wood gasification. J Cleaner Prod 13:1434–1446

Eaton AD, Clesceri LS, Rice EW, Greenberg AE (eds) (2005) Standard methods for the examination of water and wastewater (21st edn). APHA, Washington, DC, USA

Elliott DC, Hart TR, Neuenschwander GG (2006) Chemical processing in high-pressure aqueous environments. 8. Improved catalysts for hydrothermal gasification. Ind Eng Chem Res 45:3776–3781. doi:10.1021/ie060031o

Fezy JS, Spencer DF, Greene RW (1979) The effect of nickel on the growth of the freshwater diatom *Navicula Pelliculosa*. Environ Pollut 20:131–136. doi:10.1016/0013–9327(79)90065-X

Golueke CG, Oswald WJ (1963) Power from solar energy - via algae-produced methane. Sol Energy 7:86–92. doi:10.1016/0038–092X(63)90033–1

Grobbelaar JU (2004) Algal nutrition: mineral nutrition. In: Richmond A (ed) Handbook of microalgal culture: biotechnology and applied phycology. Blackwell Publishing, Oxford UK, pp 97–115

Hall DO, Mynick HE, Williams RH (1991) Cooling the greenhouse with bioenergy. Nature 353:11–12. doi:10.1038/353011a0

Hase R, Oikawa H, Sasao C, Morita M, Watanabe Y (2000) Photosynthetic production of microalgal biomass in a raceway system under greenhouse conditions in Sendai City. J Biosci Bioeng 89:157–163. doi:10.1016/S1389–1723(00)88730–7

Hu Q, Sommerfeld M, Jarvis E, Ghirardi M, Posewitz Seibert M, Darzins A (2008) Microalgal triacylglycerols as feedstocks for biofuel production: perspectives and advances. Plant J 54:621–639. doi:10.1111/j.1365–313X.2008.03492.x

Kruse A (2008) Hydrothermal biomass gasification. J Supercritical Fluids (in press). doi:10.1016/ j.supflu.2008.10.009

Kruse A, Krupka A, Schwarzkopf V, Gamard C, Henningse T (2005) Influence of proteins on the hydrothermal gasification and liquefaction of biomass 1. Comparison of different feedstocks. Ind Eng Chem Res 44:3013–3020. doi:10.1021/ie049129y

Kruse A, Maniam P, Spieler F (2007) Influence of proteins on the hydrothermal gasification and liquefaction of biomass 2. Model compounds. Ind Eng Chem Res 46(1):87–96. doi:10.1021/ie061047h

Lee L, Lustigman H (1996) Effect of barium and nickel on the growth of *Anacystis nidulans*. Bull Environ Contam Toxicol 56:985–992. doi:10.1007/s001289900142

Lustigman B, Lee LH, Khalil A (1995) Effects of nickel and pH on the growth of *Chlorella vulgaris*. Bull Environ Contam Toxicol 55:73–80. doi:10.1007/BF00212391

Luterbacher JS, Fröling M, Vogel F, Maréchal F, Tester JW (2009) Hydrothermal gasification of waste biomass. Sustainable process development using life cycle assessment. Environ Sci Technol (in press)

Mandal R, Hassan NM, Murimboh J, Chakrabarti CL, Back MH (2002) Chemical speciation and toxicity of nickel species in natural waters from the Sudbury Area (Canada). Environ Sci Technol 36:1477–1484. doi:10.1021/es015622e

Matsumura Y, Minowa T, Potic B, Kersten SRA, Prins W, van Swaaij WPM, van de Beld B, Elliott DC, Neuenschwander GG, Kruse A, Jerry A Jr (2005) Biomass gasification in near- and supercritical water: status and prospects. Biomass Bioenergy 29:269–292. doi:10.1016/j.biombioe.2005.04.006

Modell M (1985) Gasification and liquefaction of forest products in supercritical water. In: Overend RP, Milne TA, Mudge LK Jr (eds) Fundamentals of thermochemical biomass conversion. Elsevier, Amsterdam, pp 937–950

Nagase H, Yoshihara K, Okamoto Y, Murasaki S, Yamashita R, Hirata K, Miyamoto K (2001) Uptake pathway and continuous removal of nitric oxide from flue gas using microalgae. Biochem Eng J 7:241–246. doi:10.1016/S1369–703X(00)00122–4

Nakajima Y, Tsuzuki M, Ueda R (2001) Improved productivity by reduction of the content of light-harvesting pigment in *Chlamydomonas perigranulata*. J Appl Phycol 13:95–101. doi:10.1023/A:1011192832502

Nriagu JO (1980) Nickel in the environment. Wiley-Interscience, Chichester

Osada M, Hiyoshi N, Sato O, Arai K, Shirai M (2007) Reaction pathway for catalytic gasification of lignin in presence of sulfur in supercritical water. Energy Fuels 21:1854–1858. doi:10.1021/ef0701642

Peterson AA, Vogel F, Lachance RP, Fröling M, Antal MJ Jr, Tester JW (2008) Thermochemical biofuel production in hydrothermal media: a review of sub- and supercritical water technologies. Energy Environ Sci 1:32–65

Pirt SJ (1980) The effects of oxygen and carbon dioxide partial pressures on the rate and efficiency of algal (*Chlorella*) photosynthesis. Biochem Soc Trans 8:479–481

Rachlin JW, Grosso A (1993) The growth response of the green alga *Chlorella vulgaris* to combined divalent cation exposure. Arch Environ Contam Toxicol 24:16–20. doi:10.1007/BF01061084

Richmond A (2004) Biological principles of mass cultivation. In: Richmond A (ed) Handbook of microalgal culture: biotechnology and applied phycology. Blackwell Publishing, Oxford, pp 125–177

Samson R, Leduy A (1982) Biogas production from anaerobic digestion of *Spirulina maxima* algal biomass. Biotechnol Bioeng 24:1919–1924. doi:10.1002/bit.260240822

Sanz-Medel A (1998) Toxic trace metal speciation: Importance and tools for environmental and biological analysis. Pure Appl Chem 70:2281–2285. doi:10.1351/pac199870122281

Schubert M, Regler JW, Brandenberger M, Ludwig C, Vogel F (2008) Salt separation as a crucial step in continuous catalytic hydrothermal gasification of wet biomass to SNG. Poster session, 16th European Biomass Conference & Exhibition, Valencia, Spain, June 2–6, 2008

Spencer DF, Greene RW (1981) Effects of Nickel on seven species of freshwater algae. Environ Pollut Ser A 25:241–247. doi:10.1016/0143–1471(81)90086–6

Tam NFY, Wong JPK, Wong YS (2001) Repeated use of two *Chlorella* species, *C. vulgaris* and *WW* for cyclic nickel biosorption. Environ Pollut 114:85–92. doi:10.1016/S0269–7491(00)00202–5

Tsukahara K, Kimura T, Minowa T, Sawayama S (2001) Microalgal cultivation in a solution recovered from the low-temperature catalytic gasification of the microalga. J Biosci Bioeng 91:311–313. doi:10.1263/jbb.91.311

Vogel F (2009) Catalytic conversion of high-moisture biomass to synthetic natural gas in supercritical water. In: Crabtree R (ed) Heterogeneous catalysis. Handbook of Green Chemistry, vol 3. Wiley, Weinheim

Vogel F, Hildebrand F (2002) Catalytic hydrothermal gasification of woody biomass at high feed concentrations. Chem Eng Trans 2:771–777

Vogel F, Waldner MH, Rouff AA, Rabe S (2007) Synthetic natural gas from biomass by catalytic conversion in supercritical water. Green Chem 9:616–619. doi:10.1039/b614601e

Waldner MH (2007) Catalytic hydrothermal gasification of biomass for the production of synthetic natural gas. PhD thesis. ETH Zürich, Switzerland

Waldner MH, Vogel F (2005) Renewable production of methane from woody biomass by catalytic hydrothermal gasification. Ind Eng Chem Res 44(13):4543–4551. doi:10.1021/ie050161h

Waldner MH, Krumeich F, Vogel F (2007) Synthetic natural gas by hydrothermal gasification of biomass: selection procedure towards a stable catalyst and its sodium sulfate tolerance. J Supercrit Fluids 43:91–105. doi:10.1016/j.supflu.2007.04.004

Wang B (2008) CO_2 bio-mitigation using microalgae. Appl Microbiol Biotechnol 79:707–718. doi:10.1007/s00253–008–1518-y

Wang HK, Wood JM (1984) Bioaccumulation of nickel by algae. Environ Sci Tech 18:106–109

Wijffels RH (2008) Potential of sponges and microalgae for marine biotechnology. Trends Biotechnol 26:26–31. doi:10.1016/j.tibtech.2007.10.002

Wong JPK, Wong YS, Tam NFY (2000) Nickel biosorption by two chlorella species, C. vulgaris (a commercial species) and C. Miniata (a local isolate). Bioresour Technol 73:133–137. doi:10.1016/S0960–8524(99)00175–3

Worms IAM, Wilkinson KJ (2007) Ni uptake by a green alga: 2. Validation of the equilibrium models for competition effects. Environ Sci Technol 41:4264–4270. doi:10.1021/es0630341

Yoshida Y, Dowaki K, Matsumura Y, Matsuhashi R, Li D, Ishitani H, Komiyama H (2003) Comprehensive comparison of efficiency and CO2 emissions between biomass energy conversion technologies — position of supercritical water gasification in biomass technologies. Biomass Bioenergy 25:257–272. doi:10.1016/S0961–9534(03)00016–3

Zwart RWR, Boerrigter H (2005) High efficiency co-production of synthetic natural gas (SNG) and Fischer-Tropsch (FT) transportation fuels from biomass. Energy Fuels 19:591–597. doi:10.1021/ef049837w